

## CHAPTER 11

### Numerical models for simulation of the seismic behavior of RC structures—A case study

Humberto Varum, Aníbal Costa & Hugo Rodrigues

#### 11.1 INTRODUCTION

The study of the seismic vulnerability of existing buildings in urban areas with moderated/high seismic risk is of extreme importance, as well as the evaluation of its safety, according to recently proposed international codes and recommendations. The high number of buildings, particularly the modern architecture style buildings, constructed in Lisbon, Portugal, in the fifties, reveals deficient seismic behavior. In this work are presented the main results of an existing building, representative of the modern architecture style, for which the seismic vulnerability was studied.

The 3rd parcel from the Unity Type A in the Infante Santo Avenue, in Lisbon, is a singular example of a Modern Housing Project in Portugal [1]. These buildings studied are inserted in an Urban Plan initialized by Alberto José Pessoa (1919–1985), in 1947, when he joined the “Urbanization Study on the Protection Area of Palácio das Necessidades”, in *Câmara Municipal of Lisbon* (CML). In the framework of this Urban Plan, expropriated land parcels were divided for the construction of the new Infante Santo Avenue, which completed the ring created by De Gröer’s Municipal Plan (1938–1948).

Between 1949 and 1951, the CML and A. Pessoa began the urbanization process with “Before-hand Project for the residential and commercial Complex in Infante Santo Avenue Central Area”, which included 31 parcels along the new Avenue. The transverse section of the proposal reveals a volumetric composition that recreates the landscape, showing an obviously modern matrix influence. The buildings look like free objects claiming that “architecture is an awareness game, with correct and magnificent volumes linked under the light” [2], with rectilinear surfaces ‘the generators [can be seen] revealing simple forms’ [3] and with a plan order that expresses a primary determinate rhythm “with consequences extended from the simplest to the most complex, respecting the same law. A unity law is the law of a good plan: simple law and infinitely modulated” [4].

In 1954, A. Pessoa assumes a “Construction Project of the Infante Santo Avenue between the old Aqueduct and Santana à Lapa Street” and he participates, in the first work team in collaboration with the architects Hernâni Gandra and João Abel Manta, and with Jordão Vieira Dias, the engineer responsible for the structural project.

#### 11.2 UNITY TYPE A

The project of the Unity Type A is composed of a nine-storey-housing block and of a two-storey-commercial shopping block. The block plan is rectangular with 11.10 m width and 47.40 m length (Fig. 11.1). The building has the height of 8 habitation storeys plus the pilotis height at the ground floor. The “free plan” is also a reference because the house was conceived in a way to allow for flexibility of use, the 12 structural plane frames define the architectural plan of the floor type, with 6 duplex apartments. The distance between each frame’s axes is 3.80 m. Each frame is supported by two columns and has one cantilever beam on each side with a 2.80 m span, resulting in 13 modules with the rhythm: A-B-B-B-B-B-B-B-B-B-A. The two A modules are associated with two B modules making two different house types, the other B modules create 4 house types.



Figure 11.1. General views of the building block under analysis.

The structural plan presents an adequate solution to the architecture's objectives. "From the beginning of the studies, it was a permanent concern, to conceive a resistant structure concept, simple, elegant and economic. And it looks like the objective was well succeeded because since the beginning of the project elaboration there wasn't any need for changing the primitive structure".

The structural design was initially made just for vertical loads, without considering bending moments at the columns. Afterwards, new designs were developed, now considering in a simplified way the horizontal loads, corresponding to the wind, using the Cross's method in the bending moments distribution calculation. The structural engineer (J.V. Dias) does not consider seismic action in his design. He does refer to 'the low probability of simultaneous occurrence of wind and seismic actions in the same direction and at their maximum intensity'. Dias concludes that 'this building-type has superior safety conditions than the majority of Lisbon's buildings'.

Later, the importance of considering a seismic action in structural element's design was recognized was recognized. A new design project was delivered according to an article of Maria Amélia Chaves and Bragão Farinha published in "Técnica" Magazine. Horizontal forces, proportional to the floor's mass were considered in the frame nodes. But, the structural analysis was only made in the transversal direction. The structural engineer concludes that wind forces induce larger demands than seismic loads, resulting in larger cross-sections.

The Engineer Ramos Cruz, responsible for the construction, did a new design project for the 3rd parcel. He presented new calculations based on the primitive project, but he changed the original structural floor by a reinforced concrete slab. He advocates that with this continuous rigid slab, rigid diaphragm behavior is guaranteed. Another modification referred to in the design drawings is the consideration of reinforced concrete shear walls in the staircases at the ground floor. One of these referred to shear walls was intended to be developed at the total building's height. It should be noted that no RC shear walls were detected in the technical visits to the building [5].

### 11.3 DESCRIPTION OF THE STUDIED STRUCTURE

The main objectives of this work were to investigate the global behavior of a building representative of the Modern Architecture in Lisbon, and to identify their weakness under seismic loadings.

The building geometry and the dimensions of the RC elements and infill walls were given in the original project [1950–1956], and were confirmed in technical visits [6]. As already presented in previous sections, the building under study has nine storeys and the structure is mainly composed by twelve plane frames, oriented in the transversal direction (direction Y, as represented in Figure 11.2). The building behavior and safety was analyzed with a simplified plane model for each horizontal direction (X-longitudinal direction, Y-transversal direction).

The twelve transversal plane frames have the same geometry for all beams and columns. However, three different frame-types were identified, according to reinforcement detailing.

A peculiar structural characteristic of this type of buildings, with direct influence in the global structural behavior, is the empty ground storey, without infill masonry walls. Furthermore, at the ground storey the columns are 5.5 m height, while all the upper storeys have an inter-storey height of 3.0 m. Therefore, a soft-story behavior mechanism is produced at this ground floor level.



Figure 11.2. Structural system (general plan).

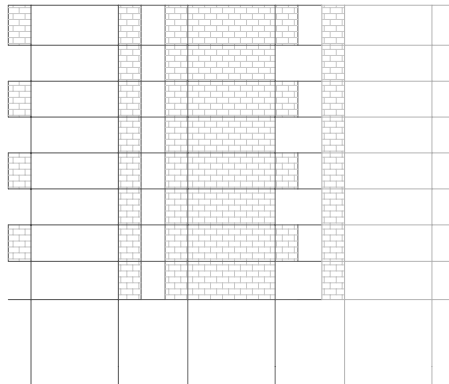


Figure 11.3. Structural model for the building analysis in the transversal direction (Y).

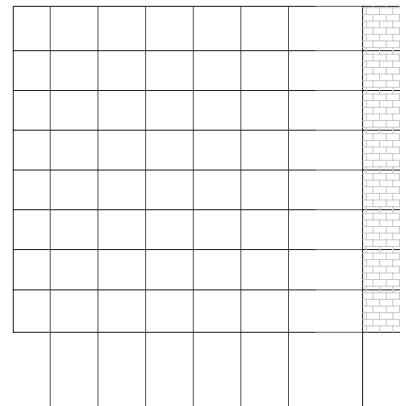


Figure 11.4. Structural model for the building analysis in the longitudinal direction (X).

In the numerical models for the analysis of the building in the two independent directions, X and Y, a concrete slab with 1.25 m width and 0.20 m thick was considered. A detailed definition of the existing infill panels, in terms of dimensions, location and materials were considered in the structural models.

For the building analysis in the transversal direction (Y), an equivalent model defined as the association of the three frame-types, interconnected by rigid strut bars, as showed in Figure 11.3 was assumed. In this global model, the geometric and mechanical characteristics of each frame are multiplied by the number of occurrences of each frame-type.

For the analysis in the longitudinal direction (X), and because of the double symmetry in the plan, just one quarter of the building was studied. The global model results a six-column-structure linked at all storey levels by RC slabs. No full-bay infill panels exist in the longitudinal direction. Therefore, an external simplified global infill masonry model was considered, as represented in Figure 11.4, connected, at storey levels, through rigid struts to the RC framed structure.

#### 11.4 MODELS DESCRIPTION

Nowadays, in the analysis of structures subjected to seismic actions, the use of non-linear behavior laws and hysteretic rules reveals a great advantage, because it makes possible a more rigorous representation of the seismic structural response.

To simulate the structural behavior of the building presented in the previous sections a computer program, PORANL, was used that contemplates the non-linear bending behavior of RC elements (beams and columns) and the influence of the infill masonry panels in the global response of the buildings.

Each RC structural element is modeled by a macro-element defined by the association of three bar finite elements, two with non-linear behavior at its extremities (plastic hinges), and a central element with linear behavior, as schematically represented in Figure 11.5.

The non-linear monotonic behavior curve of a cross-section is characterized through a tri-linear moment-curvature relationship, corresponding respectively to: the initial non-cracked concrete, concrete cracking and steel reinforcement yielding [7]. The monotonic curve is obtained using a fiber model procedure (Fig. 11.6), from: the geometric characteristics of the cross-sections, reinforcement and its location, and material properties.

The non-linear behavior of the plastic hinge elements is controlled through a modified hysteretic procedure, based on the Takeda model, as illustrated in Figure 11.7. This model developed by Costa [8] represents the response evolution of the global RC section to seismic actions and contemplates mechanical behavior effects as stiffness and strength degradation, pinching, slipping, internal cycles, etc.

To represent each infill masonry panel, an improved macro-model, based on the bi-diagonal equivalent strut model, is used (Fig. 11.8). The proposed macro-model was implemented in the non-linear structural analysis program PORANL [9]. The macro-model adopted represents the non-linear behavior of an infill masonry panel and its influence in the global RC structural behavior under static or dynamic loading.

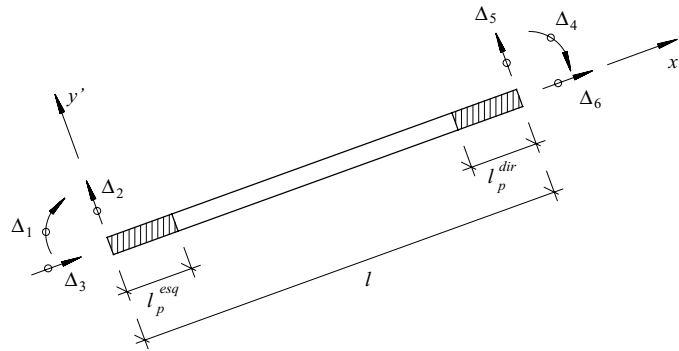


Figure 11.5. Macro-element used for the behavior simulation of reinforced concrete elements.

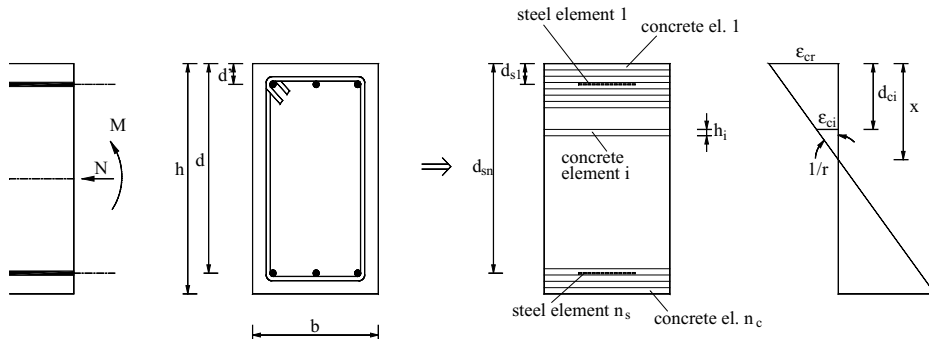


Figure 11.6. Fiber model for RC elements.

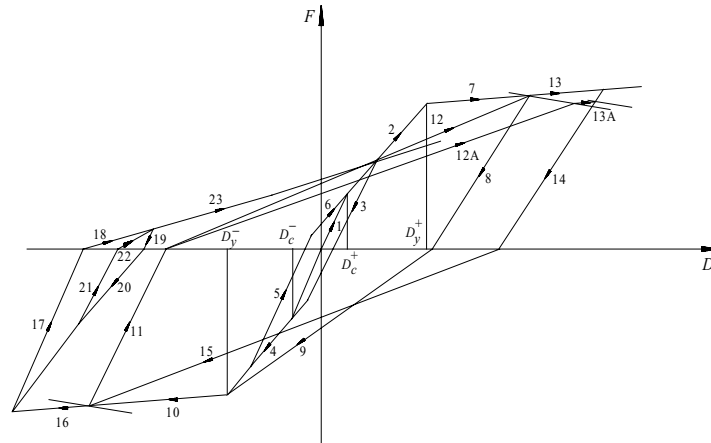


Figure 11.7. Hysteretic model for RC elements [4].

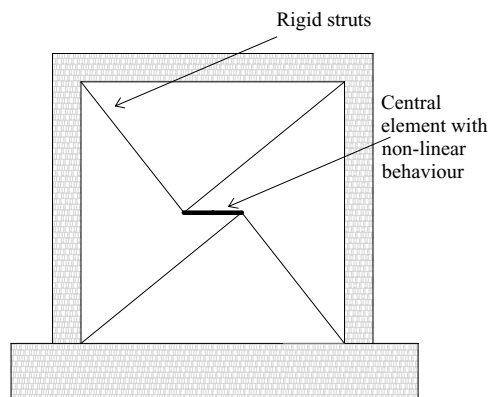


Figure 11.8. Infill masonry panel macro-model.

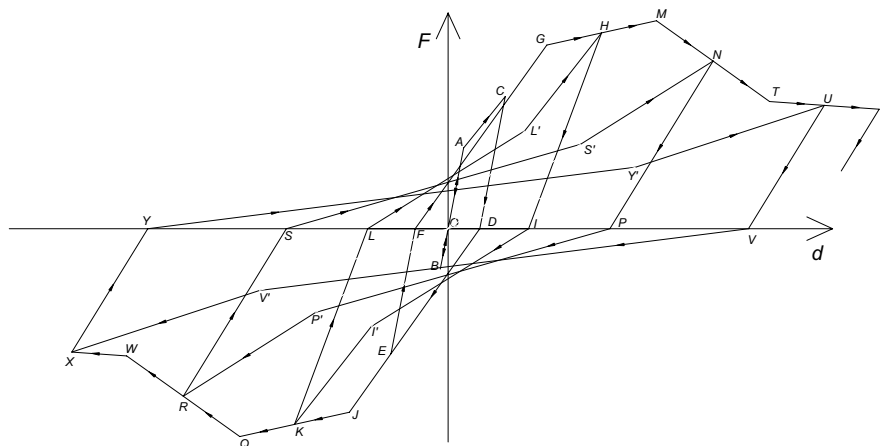


Figure 11.9. Hysteretic model (non-linear monotonic curve and hysteretic rules) for infill masonry panels [7].

The monotonic behavior curve of each panel depends on the panel dimensions, eventual openings (dimensions and position), material properties (bricks, mortar, and plaster), quality of the handwork, and interface conditions between panel and the surrounding RC elements. The behavior curves can be obtained from empirical expressions or from experimental results [10, 11].

The non-linear behavior of the infill masonry panels subjected to cyclic loads is controlled through a hysteretic procedure and rules, illustrated in Figure 11.9, and represents the non-linear mechanical effects as stiffness and strength degradation, pinching, and internal cycles.

### 11.5 STATIC LOADS, MASSES AND DAMPING

For the numerical analyses, constant vertical loads distributed on beams were considered in order to simulate the dead load associated to the self-weight of RC structural elements, infill walls, finishing's, and the correspondent quasi-permanent value of the live loads, totalizing a value of  $8.0 \text{ kN/m}^2$ .

The mass of the structure was assumed concentrated at storey levels. Each storey has a mass, including the self-weight of the structural and non-structural elements, infill walls and finishings, and the quasi-permanent value of the live loads, of about 4 Mtons. For the dynamic analysis, the storey mass is assumed to be uniformly distributed on the floors.

For each building model, a Rayleigh damping matrix, with 1% damping ratio for the first two natural modes was computed.

### 11.6 NATURAL FREQUENCIES AND MODAL SHAPES

A first validation of any structural numerical model can be achieved comparing the experimentally measured and the analytically estimated natural frequencies. Table 11.1 lists the four first natural frequencies computed, for the building under analysis and for each direction (X and Y).

To validate the numerical model of the building, in the two independent directions, the first natural structural frequency was measured with a seismograph using only the ambient vibration. The measured first frequency for each direction is indicated in Table 11.1 (in brackets).

A good agreement was found between the experimentally measured frequencies (1.17 Hz for the longitudinal direction and 1.56 Hz for the transversal direction [12]) and the frequencies estimated with the structural numerical models (1.08 Hz for the longitudinal direction and 1.75 Hz for the transversal direction), which constitutes the first validation of the numerical model developed. In Figure 11.10 the first natural mode shapes calculated for each direction are represented.

From the analysis of the first shape vibration modes, in both directions, it is clear that seismic actions will tend to induce a soft-storey mechanism response. This conclusion will be confirmed with the earthquake response analysis in the next sections.

Table 11.1. Natural frequencies (directions X and Y).

Frequencies	Direction	
	Longitudinal X (Hz)	Transversal Y (Hz)
1st	1.08 (1.17)	1.75 (1.56)
2nd	5.67	6.41
3rd	6.32	8.14
4th	8.10	8.80

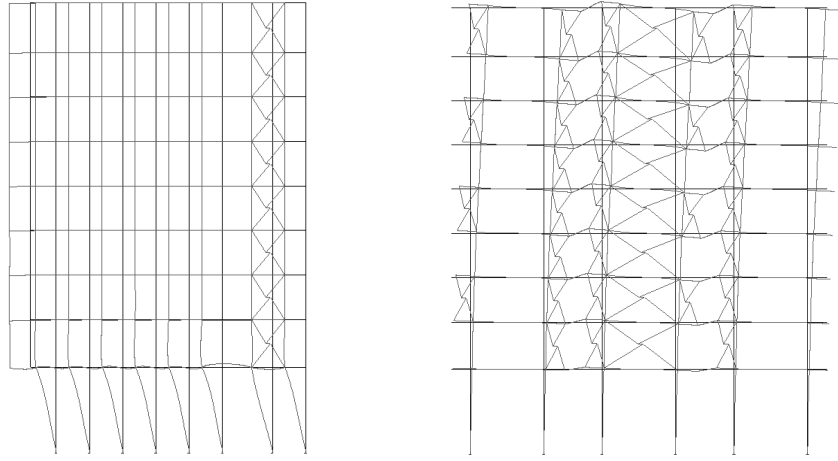


Figure 11.10. Natural vibration shape modes ( $f_{1,X} = 1.08$  Hz and  $f_{1,Y} = 1.75$  Hz).

Table 11.2. Reference earthquake action (peak ground acceleration and corresponding RP).

Return period (years)	Peak ground acceleration ( $\times g$ )
73	0.091
475	0.222
975	0.294
2000	0.380
3000	0.435
5000	0.514

## 11.7 EARTHQUAKE INPUT MOTIONS

Three artificial earthquake input series were adopted for the seismic vulnerability analysis of the building. The first series (A) was artificially generated for a medium/high seismic risk scenario in Europe [13], for various return periods (RP) (Table 11.2). The second and third series (B and C, respectively) were generated with a finite fault model for the simulation of a probable earthquake in Lisbon [14], calibrated with real seismic actions of low intensity measured in the region of Lisbon (see earthquake examples in Figures 11.11 to 11.13). The peak ground acceleration values for each return period are presented in Table 11.2.

## 11.8 RESULTS ANALYSIS

As observed in the free vibration shape modes, the structural response of the building, in both directions, clearly denotes typical soft-storey mechanism behavior (at the ground floor level). This structural behavior leads to large storey deformation demands at the first storey, while the upper storeys remain with very low deformation levels.

In Figures 11.14 and 11.15 are illustrated, for the longitudinal and transversal direction, respectively, the numerical results in terms of envelop deformed shape, maximum inter-storey drift, and maximum storey shear, for each earthquake input motion of the series A (73, 475, 975, 2000, 3000, 5000 years return period).

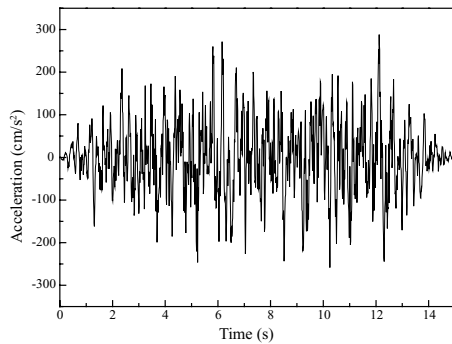


Figure 11.11. Accelerogram A.

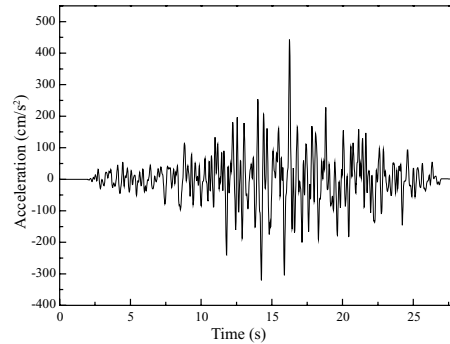


Figure 11.12. Accelerogram B.

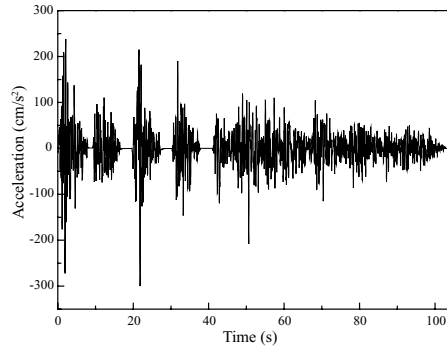


Figure 11.13. Accelerogram C.

From the analysis of the results in terms of building envelop deformed shape and inter-storey drift profile, for both directions, it can be concluded that the deformation demands are concentrated at the first storey level. In fact, the absence of infill masonry walls at the ground storey and the larger storey height (5.50 m for the 1st storey and 3.00 m for the upper storeys), induces an important structural irregularity in elevation, in terms of stiffness and strength.

For all the structural elements (columns and beams), and for all the seismic input action levels, the shear force demand assumes a value inferior to the corresponding shear capacity, which confirms its safety in shear.

#### 11.8.1 *Vulnerability curves*

This section compares, for the three earthquake series of input motions, the vulnerability curves in terms of maximum drift at ground storey, maximum 1st storey shear and maximum top displacement, for the longitudinal and transversal directions.

In Figures 11.16 and 11.17 the vulnerability curves are plotted for the longitudinal and transversal directions, in terms of the maximum 1st storey drift, obtained from the numerical analysis. Results show that, for the 1st storey, the maximum inter-storey drift demand for the longitudinal direction is larger than for the transversal, being the most vulnerable the longitudinal direction of the building.

In Figures 11.18 and 11.19 the vulnerability curves are represented in terms of maximum 1st storey shear force. In Figures 11.20 and 11.21 the obtained vulnerability curves are represented in



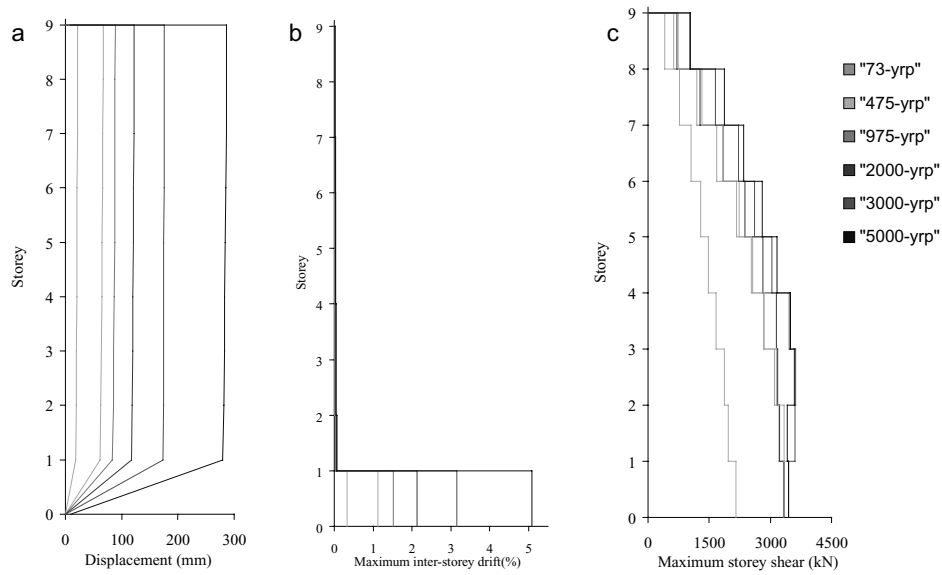


Figure 11.14. Results for the longitudinal direction (X) and earthquakes of the series A: (a) envelop deformed shape; (b) maximum inter-storey drift profile; (c) maximum shear profile.

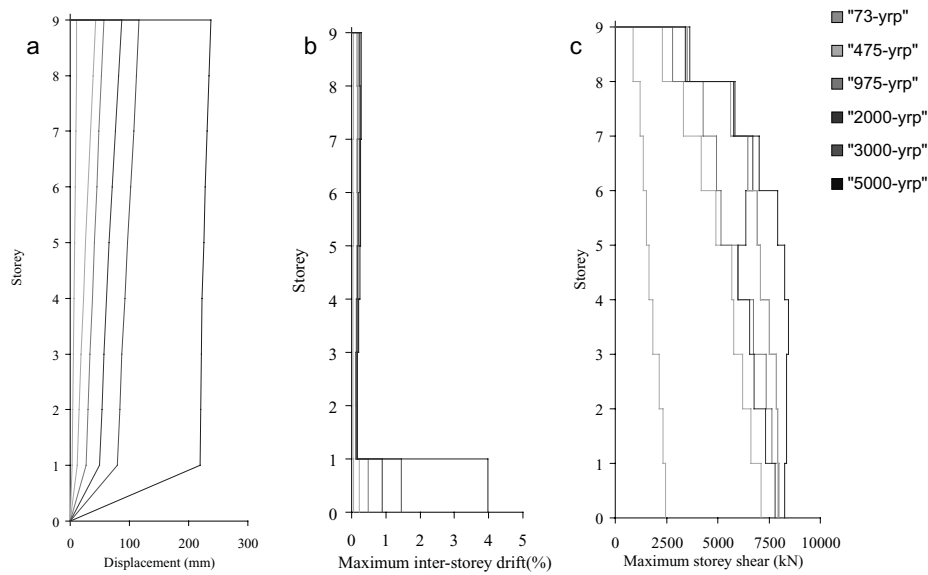


Figure 11.15. Results for the transversal direction (Y) and earthquakes of the series A: (a) envelop deformed shape; (b) maximum inter-storey drift profile; (c) maximum shear profile.

terms of maximum top displacement. Shear demand at 1st storey does not increase for earthquake input actions larger than the corresponding to the return period of 475 years, inducing demands increasing just in terms of deformation, as can be observed in the results in terms of 1st storey drift and top displacement.

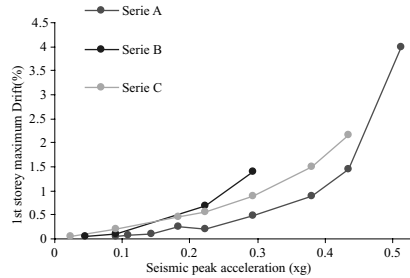


Figure 11.16. 1st storey maximum drift vs peak acceleration (transversal direction Y).

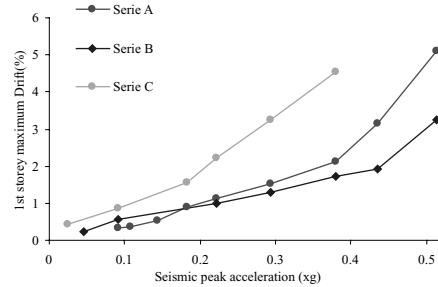


Figure 11.17. 1st storey maximum drift vs peak acceleration (longitudinal direction X).

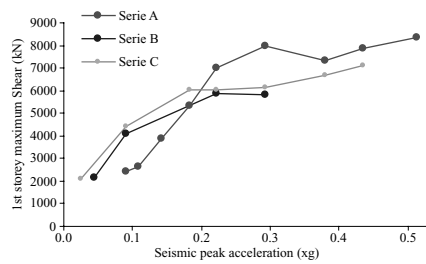


Figure 11.18. 1st storey maximum shear vs peak acceleration (transversal direction Y).

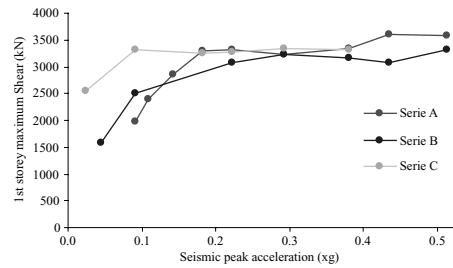


Figure 11.19. 1st storey maximum y shear vs acceleration (longitudinal peak direction X).

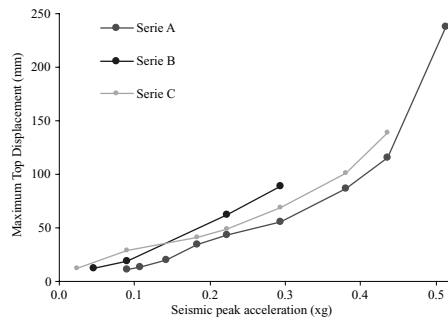


Figure 11.20. Maximum top displacement vs peak acceleration (transversal direction Y).

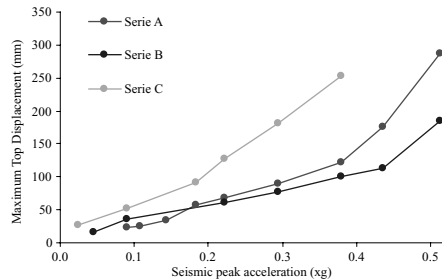


Figure 11.21. Maximum top displacement vs peak acceleration (longitudinal direction X).

### 11.8.2 Building seismic safety assessment

As presented in previous sections, for each direction (X and Y), the building structure was analyzed for three series of earthquakes, in order to estimate deformation demands, and consequently damage levels for each input earthquake intensity.

The obtained results allow verifying the safety according to the specified hazard levels, for example, the proposed in VISION-2000 [13] and ATC-40 [14] recommendations. In Tables 11.3 and 11.4 the acceptable inter-storey drift limits are presented for each structural performance level, according to the ATC-40 [14] and in VISION-2000 [13] proposals, respectively.

Table 11.3. Inter-storey drift limits according to the ATC-40 [14].

	Performance level			
	Immediate occupancy	Damage control	Life safety	Structural stability
Drift limit	1%	1–2%	2%	$0.33 \frac{V_i}{P_i} \approx 7\%$

Table 11.4. Inter-storey drift limits according to the VISION-2000 [13].

	Performance level			
	Fully operational	Operational	Life safe	Near collapse
Drift limit	0.2%	0.5%	1.5%	2.5%

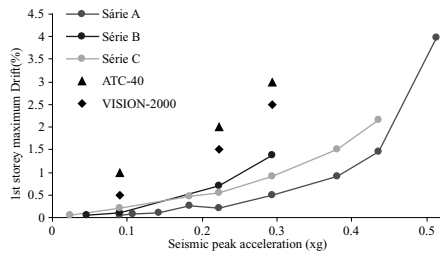


Figure 11.22. Maximum 1st storey drift vs peak acceleration and safety limits (transversal direction Y).

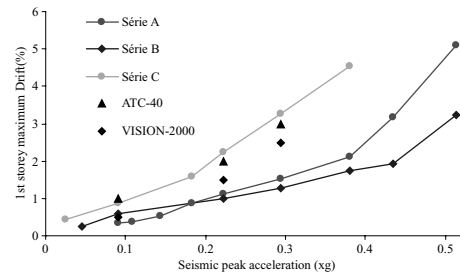


Figure 11.23. Maximum 1st storey drift vs peak acceleration and safety limits (longitudinal direction X).

In Figures 11.22 and 11.23 the vulnerability functions are represented in terms of maximum 1st storey drift, already presented in the previous section, with indication of the safety limits proposed at the ATC-40 [14] and VISION-2000 [13] recommendations (as summarized in Tables 11.3 and 11.4, respectively).

Comparing the maximum storey drift demands with the safety limits proposed at the ATC-40 [14] and VISION-2000 [13] recommendations, it can be concluded that the building safety is guaranteed in the transversal direction (Y), for the three earthquake input series considered. For the longitudinal direction (X), the safety is guaranteed for earthquake series A and B, but not for C series.

## 11.9 STUDIED RETROFITTING SOLUTION

For the improvement of the seismic response of the building under study, a retrofitting solution, intending to reduce the soft-storey mechanism was analyzed. This solution aims to reduce the deformation demand at the ground floor level. More specifically an X-bracing system with an associated shear-link dissipation device (see Figures 11.24 and 11.25) was produced, which can increase stiffness and damping of the building and consequently reduce the deformation demands. This retrofitting solution is based on a solution experimentally studied by Varum [9]. The adoption

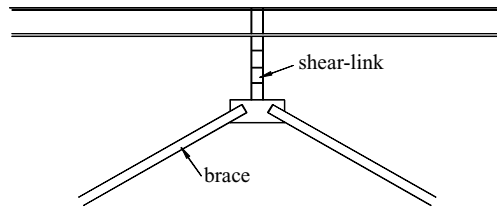


Figure 11.24. Shear-link (energy dissipation device).

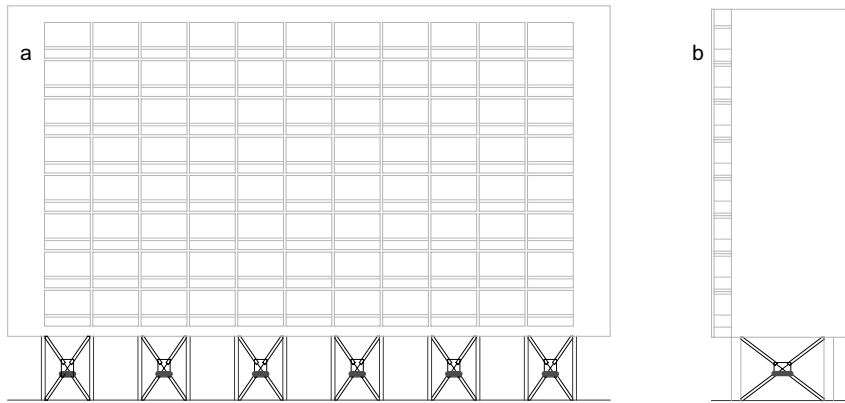


Figure 11.25. Location of the shear links: (a) Longitudinal direction; (b) Transversal direction.

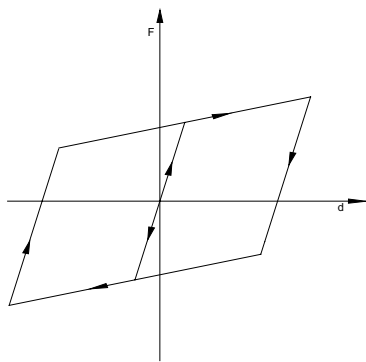


Figure 11.26. Hysteretic behavior model proposed for the shear-link (implemented in VisualANL).

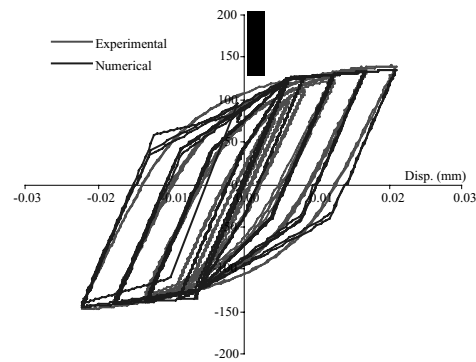


Figure 11.27. Calibration of the numerical model for the device cyclic behavior.

of an X-bracing retrofitting solution was proposed due to the efficiency in reducing the deformation demands of the building, and on other hand due to the fact that this retrofitting solution does not significantly change the architecture layout (only applied at the ground floor) (Fig. 11.25). Many alternatives for the location of the bracings can be chosen, in the central or external bays (Fig. 11.25). A new numerical model in the computational program, VisualANL, was developed and implemented to simulate the non-linear behavior of the device. The proposed model was implemented in the computer program and calibrated with experimental results on a full-scale cyclic test in a frame retrofitted with the same dissipative device [9]. The hysteretic behavior

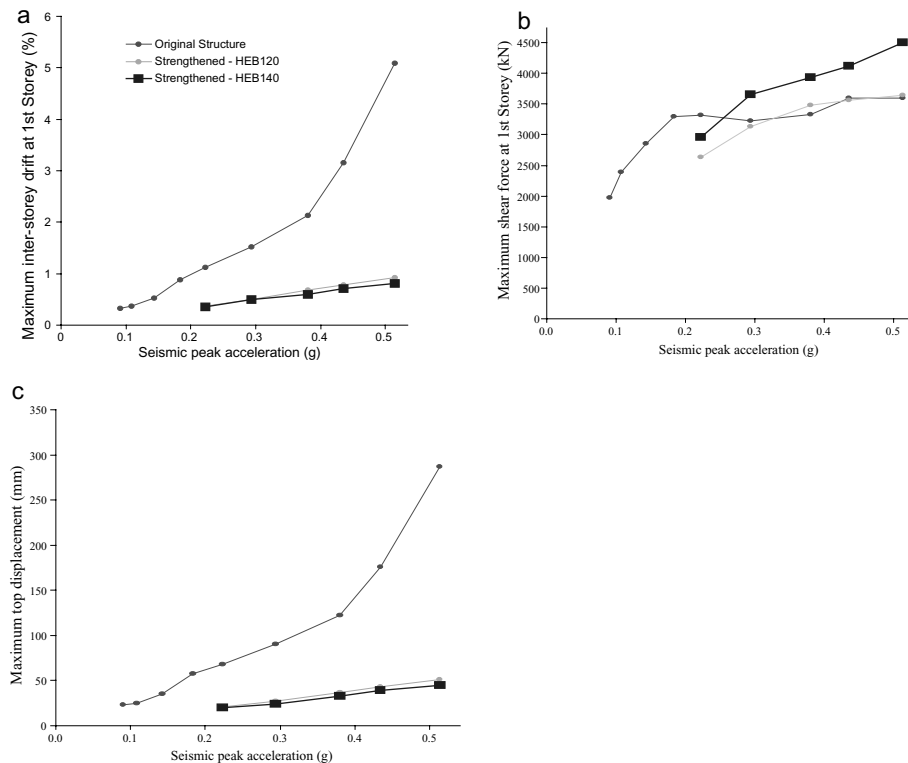


Figure 11.28. Results for the transversal direction (Y): (a) 1st storey maximum drift; (b) 1st storey maximum shear; (c) Maximum top displacement.

and rules and the results of the calibration analysis are presented in Figures 11.26 and 11.27, respectively.

With the proposed retrofitting solution for the longitudinal direction, two different solutions (solution A: HEB140,  $L = 60$  cm; and, solution B: HEB120,  $L = 60$  cm) were tested. The results were evaluated in terms of maximum 1st storey drift, maximum base shear and maximum top displacement, as presented in Figure 11.28. From the observation of these first results, the following conclusions can be accomplished about the retrofitting efficiency: (1) a pronounced reduction in terms of deformation demands (inter-storey drift and top-displacement demands); (2) a similar deformation demands reduction level for both retrofitting solutions; (3) an increase of the global shear demands at the base for shear-link HEB140; (4) with the retrofitting scheme studied, a soft-storey mechanism is prevented, even for significant acceleration levels (0.5 g). However, the strengthening solution proposed must be optimized in terms of number and location of the shear-links, and their properties as strength and elastic stiffness.

## 11.10 CONCLUDING REMARKS

The global structural safety of a modern architecture building at the Infante Santo Avenue, in Lisbon, was investigated. Although the results indicate the building safety for the Basic Objectives according to the international seismic recommendations (ATC-40 [14] and VISION-2000 [13]), it should be pointed out that additional analyses have to be performed. The input motion earthquakes adopted for these analyses can be not fully representative of the possible seismic action in Lisbon.

In other way, the level of structural damage does not depend only on the peak ground acceleration of the earthquake. Additional analyses should be performed using other earthquake input motions.

Shear capacity was verified for all the input motions. However, the model adopted for these analyses does not consider the geometric non-linearity, which can increase significantly the moments in columns and global storey lateral deformations (drifts). Therefore, to guarantee the seismic safety of the building, it is judged focal to verify the results using a model that considers the second order effects (geometrical non-linearities). Finally, it was analyzed a simple and economic seismic retrofitting solution, which is able to reduce the seismic vulnerability associated to the structural behavior and deficiencies of typical existing buildings of modern architecture style, as showed by the first results. However, further analyses to optimize the ratio cost/efficiency of the proposed retrofitting solution should be performed.

## REFERENCES

1. Tostões, A.: *Os verdes anos na arquitectura Portuguesa dos anos*. Faculty of Architecture of University of Porto, Porto, Portugal, 1997.
2. Tostões, A.: *Arquitectura moderna portuguesa*. IPPAR, Lisbon, Portugal, 2004.
3. Le Corbusier: *Vers une architecture*. Flammarion, Paris, France, 1923.
4. Varum, H.: *Modelo numérico para análise de pórticos planos de betão armado*. MSc Thesis, Civil Engineering Department, University of Porto, Porto, Portugal, 1996.
5. Costa, A.G.: *Análise sísmica de estruturas irregulares*. PhD Thesis, Civil Engineering Department, University of Porto, Porto, Portugal, 1989.
6. Miranda, L., Rodrigues, H., Fonseca, J. and Costa, A.: Inspection report to the Infante Santo Complex, Porto, Portugal, 2005.
7. Rodrigues, H., Varum, H. and Costa, A.: Numeric model to account for the influence of infill masonry in the RC structures behavior. *Proceedings Congreso Métodos Numéricos en Ingeniería*, 2005.
8. Zarnic, R. and Gostic, S.: Non-linear modelling of masonry infilled frames. *Proceedings 11th European Conference on Earthquake Engineering*, Paris, France, ISBN 90 5410 982 3, A.A. Balkema, Rotterdam, 1998.
9. Varum, H.: *Seismic assessment, strengthening and repair of existing buildings*. PhD Thesis, Department of Civil Engineering, University of Aveiro, Aveiro, Portugal, 2003.
10. Infante Santo residential building (Block 3), Drawings and Descriptive and Justificative Memoir, 1950–1956.
11. Carvalho, A., Campos-Costa, A. and Oliveira, C.S.: A stochastic finite—fault modelling for the 1755 Lisbon earthquake. *Proceedings 13th World Conference on Earthquake Engineering*, Vancouver, BC, Canada, 2004.
12. Carvalho, E.C., Coelho, E. and Campos-Costa, A.: Preparation of the full-scale tests on reinforced concrete frames—Characteristics of the test specimens, materials and testing conditions. ICONS report, Innovative Seismic Design Concepts for New and Existing Structures, European TMR Network —LNEC, Lisbon, Portugal, 1999.
13. SEAOC: Performance based seismic engineering of buildings, Part 2: Conceptual framework. Vision 2000 Committee, Structural Engineers Association of California, Sacramento, CA, 1995.
14. Applied Technical Council: ATC-40: Seismic evaluation and retrofit of concrete buildings. Applied Technical Council, California Seismic Safety Commission, Report SSC 96-01 (two volumes), Redwood City, CA, 1996.